PAPER • **OPEN ACCESS**

Rock mass geomechanical properties to improve rockfall susceptibility assessment: a case study in Valchiavenna (SO)

To cite this article: G Bajni *et al* 2021 *IOP Conf. Ser.: Earth Environ. Sci.* **833** 012180

Rock mass geomechanical properties to improve rockfall susceptibility assessment: a case study in Valchiavenna (SO)

G Bajni[1], C A S Camera[1], A Brenning[2] and T Apuani[1]

[1]Dipartimento di Scienze della Terra "A. Desio", Università degli Studi di Milano, Via Luigi Mangiagalli, 34, 20133 Milan, Italy.

[2]Department of Geography, Friedrich Schiller University Jena, 07743 Jena, Germany.

greta.bajni@unimi.it

Abstract. The overarching goal of the study is to develop a rockfall susceptibility map for Valchiavenna (SO), located in the Italian Central Alps. The approach was two-fold: the first part of the work consisted of developing geomechanical maps, which are relevant to rock mass instability, whilst the second part was aimed to the implementation of the obtained geomechanical maps as predictors in a statistically based rockfall susceptibility model. The chosen target variables, collected in an available geomechanical field surveys database, were Joint Volumetric Count (J_v), the equivalent hydraulic conductivity (K_{eq}), and weathering index (W_i). The available dataset was updated with several new geomechanical surveys, whose locations were chosen through the application of the Spatial Simulated Annealing algorithm. Based on this updated and homogenised dataset, the target properties were regionalized using different deterministic, geostatistical and regression techniques, comparing performance and error metrics resulting from a leave-one-out cross-validation procedure. Regionalization results of the target variables showed different reliability degrees. To improve the hydrogeological processes understanding on another spatial scale, an infiltration density map was prepared, based on field-mapped elements prone to infiltration- Rockfall susceptibility modelling was performed using Generalized Additive Models (GAM), along with the more commonly used topographic predictors. Model performance is assessed using both non-spatial and spatial k-fold cross-validations to estimate the area under the receiver operating characteristic curve (AUROC). Predictor smoothing functions and deviance explained were analysed in order to assess the influence of the geomechanical predictors on the model. The geological-geomorphological plausibility of the susceptibility map including geomechanical predictors was assessed by a comparison with the only topography-based susceptibility map. Model results showed reliable rockfall discrimination capabilities (mean AUROC>0.7). Rockfall data for model training and testing were extracted from the IFFI (Inventario dei Fenomeni Franosi in Italia) inventory and updated with additional field-mapped rockfalls. A potential inventory bias in the IFFI inventory was observed by comparing performance and predictors behaviour of models built with and without the additional rockfalls.

1. Introduction

Rockfalls are a common type of instability, deeply affecting human society and infrastructures in mountainous environments [1]. While it is clear that failure probabilities for individual vertical cliff differ from each other, understanding which areas of a steep cliff are more likely to originate rockfalls–

and why even close rock walls behave differently - still remains an open challenge [2]. Indeed, where climate and topography are similar, variability in rockfall susceptibility is linked to differences in rock geomechanical characteristics, the local stress state, and variations in hydrogeologic conditions [3].

Traditionally, rockfall runout is more frequently and extensively investigated than rockfall susceptibility [4], which could result in too generic interpretations if including only topographic predictors, as these phenomena reflect a complex interplay of numerous processes acting at different spatial-temporal scales [5]. On the other hand, acquiring geo-structural and geomechanical data for regional scale investigations is time consuming and these properties are difficult to interpolate [6]. Some authors regionalized some geomechanical properties such as Joint Volumetric Count [7] Rock Mass Rating [8,9,10] and joint spacing [11] over large areas. However, the available starting geomechanical datasets are rare and sometimes not suitable for interpolation, as prepared in relation to local geotechnical problems or clustered close to roads and infrastructures. An approach to overcome these problems could be designing optimal sampling schemes to update, or create, new geomechanical datasets in the area of interest, saving time and costs related to field survey. Several methods for sampling design are available in digital soil mapping literature [12] which nonetheless are not frequently used for geomechanical applications.

In recent years, rockfall susceptibility modeling with statistical and machine learning methods have been increasingly and successfully applied [5,13,14]; however, rock-mass related characteristics are mostly included in the analysis as distance to fault or joints orientation in respect to slope gradient. Where possible, other geomechanical properties influence on rockfall activity should be tested, which need to be consistent with the volume and scale of the investigated instability type. Above all, fracturing degree, rock mass weathering and hydrogeological properties are traditionally recognized as the most important parameters describing rock mass mechanical conditions. Moreover, these characteristics are included in the most common classification systems (e.g. RMR [15] and Q-System [16]), in turn influencing rock mass strength and instability likelihood.

This study was three-fold: firstly, an available dataset for Chiavenna Valley (SO, Italy), was updated and revised by optimizing the selection of additional sampling points and execution of the geomechanical surveys. Secondly, three representative properties, Joint Volumetric Count (J_v), rock-mass weathering index (W_i) and rock-mass equivalent permeability (K_{eq}) were selected and calculated starting from geomechanical field-surveyed metrics and regionalized over the study area. Finally, the obtained geomechanical maps were implemented as predictors in a rockfall susceptibility model performed using Generalized Additive Models (GAM), already successfully applied in susceptibility studies [17]. To our knowledge, this research represents the first attempt of including outcrop-scale geomechanical properties in this type of analysis.

2. Study Area

Chiavenna Valley (Provence of Sondrio) is located in the Italian Central Alps (figure 1a) and consists of two orthogonal branches: San Giacomo valley (N-S oriented), and Bregaglia valley (E-W oriented), both connecting Italy to Switzerland. The geological setting of San Giacomo Valley is characterized by sub-horizontal NE verging tabular gneissic bodies, i.e. Tambò and Suretta Pennidic nappes, separated by the Mesozoic sedimentary cover of Spluga Syncline [8]. The structural contact between Tambò and Suretta nappes, marked by a NE gently dipping schistosity, also extends through the northern slope of Bregaglia Valley, whereas its southern slope is characterized by the presence of the granulite-migmatite Gruf Complex in structural contact with the ophiolitic Chiavenna Unit [18]. The structural framework of the area reflects the directions of some main tectonic alignments: a WNW-ESE system related to the Insurbric Line, a NW-SE system linked to the Forcola Fault and a NE-SW system associated with the Engadine Line [8]. With this same latter direction, the sub-vertical mylonitic zone of the Gruf Line [18] characterizes the southern slope of Bregaglia Valley. The interplay between tectonic processes and post-glacial debuttressing, following the retreat of Engadine-Bregaglia and San Giacomo glaciers [19], is crucial in defining the actual slope dynamics in the study area.

3. Materials and methods

3.1. Available data

A geomechanical dataset of 128 survey points, with different levels of information regarding both primary variables (e.g. Joint Roughness Coefficient JRC, Schmidt Hammer rebounds, joints spacing, orientation and aperture) and derived variables (e.g. Palmstrom's J_v, RMR, GSI) was available for the study area (database of geoengineering research group of the Dept. of Earth Sciences, Università degli Studi di Milano). The Digital Terrain Model (DTM) at a 5 m x 5 m resolution, mainly based on the DBTR (Topographic Regional Data Base) project and LIDAR surveys (2008-2009; 2010-2011; 2013-2015), was freely available on the Lombardy Region Geoportal (http://www.geoportale.regione.lombardia.it/). Rockfall inventory is based on the freely available IFFI dataset (Inventario Fenomeni Franosi in Italia - https://www.progettoiffi.isprambiente.it/), recording both rockfall source points and deposits. This dataset was updated by several new rockfalls scarps and deposits, covering also remote areas, mapped during detailed geomorphological-structural field surveys, integrated with remote sensing, carried out from 2002 to 2018 in the framework of Unimi Master's Degree Theses in Earth Science and by [20]. The geomechanical dataset and rockfall inventory locations are reported in figure 1c.

3.2. Sampling strategy and field work

The pre-existing geomechanical dataset was found to be quite heterogeneous, sometimes incomplete, and clustered along main roads (i.e. accessible areas), thus not suitable for spatialization purposes. For this reason, the model-based Spatial Simulated Annealing [12, 21] algorithm was adopted to select locations to update the available geomechanical dataset. To optimize the coordinates of the new sampling points, SSA procedure involved the minimization of a prediction error variance associated to pre-existing points. As J_v was the only target property collected in each survey point, a preliminary spatialization of this property by means of ordinary kriging was performed and the associated variance was used as the minimization criterion to obtain 25 new survey locations. Detailed geomechanical field surveys were performed in the points identified – and some previous data were contextually revised – according to the International Society of Rock Mechanics (ISRM) suggested methods. Due to the high mountain environment involved in the field work, in few cases the exact selected points were unreachable; in such situation more easy-reachable areas with similar characteristics were alternatively selected.

3.3. Target properties calculation and regionalization

Alongside J_v, representing the rock mass fracturing degree, W_i and K_{eq}, respectively representative of weathering conditions and equivalent permeability of rock masses were calculated for each new and revised sampling point too. Wi was calculated as the ratio between JCS (Joint Compressive strength) on natural and abraded joint surfaces. JCS values were obtained by converting Schmidt hammer rebound measures through the table proposed by [22]. Rebounds can be associated to surface exposure age and rock weathering as found by some authors e.g. [23]. K_{eq} was calculated following [24,25]:

$$K_{eq} = \left(k_{xx}k_{yy}k_{zz}\right)^{\frac{1}{3}} \quad (1)$$

where k_{xx}, k_{yy} and k_{zz} represent the principal components of the permeability tensor $\underline{K}$:

$$\underline{K} = g(12v)^{-1}\sum_{i=1}^{N} f_i e_i{}^3\,[I - \vec{n}\otimes\vec{n}] \quad (2)$$

where g is the gravity acceleration, ν is the kinematic viscosity of water, N is the total number of discontinuities sets, f is the average frequency of the i-set (m^{-1}), e is the average hydraulic aperture of the i-set (m), I is the identity matrix and n is the dimensionless unitary vector normal to the average plane of the i-set.

Susceptibility modeling requires spatially distributed predictors; therefore, each target property was interpolated in the whole study area by comparing different deterministic (Inverse Distance Weighting, Thin Plate Spline), geostatistical (Ordinary Kriging, Kriging with external drift) and regression (Multiple Linear Regression, Geographically Weighted Regression) techniques. The output maps associated to the most reliable technique were adopted as predictors. Uncertainty was assessed through a leave-one-out cross-validation (LOO-CV) calculating both performance and error metrics (respectively correlation coefficient *R* between modeled and observed values, and NMRSE) and through an analysis of the geomorphological plausibility of the variable values distribution. Regionalization was performed at 50 m x 50 m and a bilinear interpolation for resampling at DTM resolution was then applied.

3.4. Rockfall susceptibility modelling

For rockfall susceptibility modelling GAM were adopted, mostly because they allow predictor-response relationships interpretability [17,26]. Modelling was conducted in R environment using the *mgcv* package [27] for GAM implementation. As every susceptibility model, both a binomial response variable and predictors were necessary. The response variable is represented by rockfall presence and absence. While the presence was represented by the rockfall inventory, rockfall absence locations were extracted randomly on a "eligible" area: urban areas, glaciers and water bodies, quaternary deposits and every point in a 80 m buffer from rockfalls scarps were masked. Predictors were the combination of DTM-derived topographic variables i.e. elevation, slope, aspect - included as northness=cos(aspect) and eastness=sin(aspect) -, profile curvature, plan curvature, Topographic Wetness Index (TWI) and the regionalized geomechanical predictors. To include the hydrogeological characterization at a different spatial scale, the infiltration density predictor was derived too. It was calculated as the density of geomorphological-structural elements prone to infiltration such as regional lineaments, trenches and counterscarps, sinkholes.

Model performance was assessed using both non-spatial and spatial k-fold cross-validations (nsCV and sCV, respectively) to estimate the area under the receiver operating characteristic curve (AUROC). Furthermore, predictor smoothing functions and deviance explained were analysed in order to assess the importance of the geomechanical predictors in the model. With this same purpose, two models were tested and compared: a topography-based model and a topographic-geomechanical model. Shrinkage for variable selection was adopted, which means that predictors with low or no influence on the model would be penalized out of the model; penalized topographic predictors were not further considered in the successive geomechanical model. Finally, a potential inventory bias in the IFFI inventory was also assessed by comparing model performance and predictor behaviour of the topographic-geomechanical model built with and without the new mapped rockfalls.

4. Results

4.1. Regionalization of geomechanical properties

Ordinary kriging performed on J_v before updating the geomechanical dataset by means of SSA deriving points resulted in an anisotropic variogram with a maximum range direction in the SW-NE direction, approximately parallel to the main schistosity dip direction. Figure 1b shows the associated kriging variance, while figure 1c shows the SSA selected points and the survey locations performed in addition to the old dataset.

Since not statistically significant (p-val>0.05) strong linear relationships were observed between target properties and environmental covariates (i.e. elevation, slope, aspect variables, longitude and latitude), MLR and KED were discarded.

After carrying out the additional surveys, J_v regionalization best results were obtained by an ordinary kriging with an anisotropic variogram in the NW-SE direction. This change in the maximum range direction could be explained as a stronger relationship with the joint family related to the Forcola fault, only revealed by the new field surveys. LOO-CV correlation between observations and predictions

increased from 0.43 to 0.49 and the associated variance globally decreased in comparison to the pre-field survey (figure 1d).

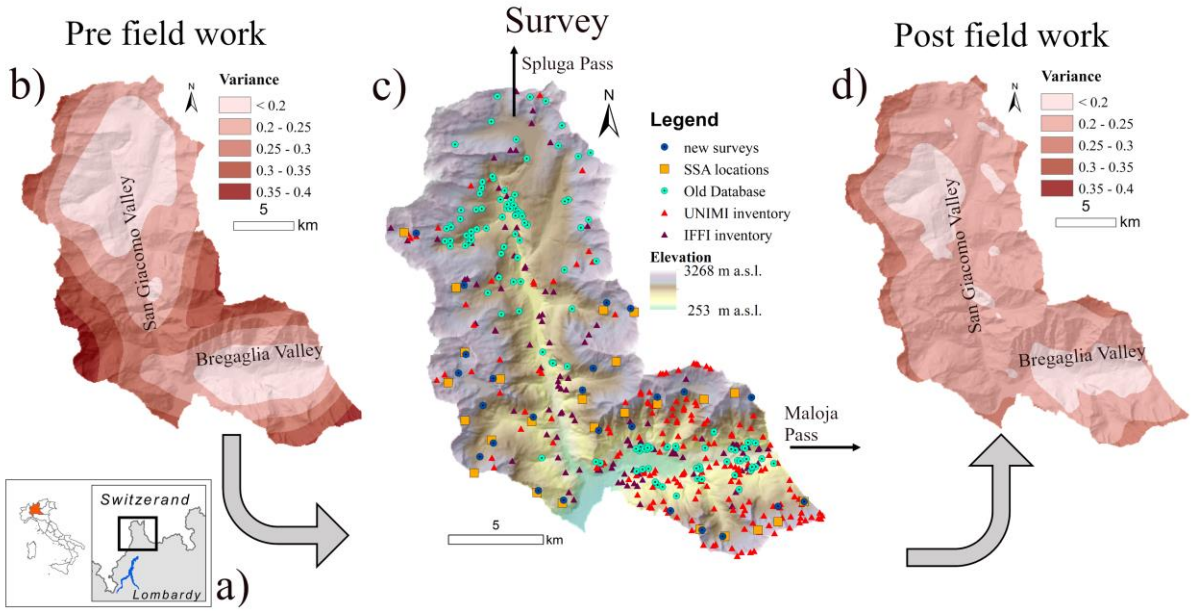

Figure 1. (a) Study area location; (b) J_v kriging variance pre-field work; (c) Geomechanical and rockfall spatial distribution; (d) J_v kriging variance pre-field work.

Only a very slight increase in variance resulted locally in the NE part of San Giacomo Valley, due to the different anisotropy direction of the variogram. This result demonstrates that the sampling algorithm and the consequent field survey reduced the uncertainties related to the regionalization of this index.

For the weathering index, the best performances were obtained adopting a GWR technique; however, the distribution of the values was considered unrealistically homogeneous in respect to the variability observed in the field. For this reason, the map associated with the isotropic ordinary kriging, with only a slight decrease in the performance but with a more reliable spatial variability and complexity of the index, was selected. The K_{eq} index resulted in the poorest performance results, and this uncertainty needs to be accounted for and communicated to potential users. The best results were obtained using a TPS method including altitude as covariate. Table 1 reports performance and error metrics for the different interpolation techniques applied to each geomechanical property.

Table 1. Geomechanical properties interpolation performance and error metrics.

	J_v			W_i			K_{eq}		
Method	*R*	*NMRSE*	*Covariates*	*R*	*NMRSE*	*Covariates*	*R*	*NMRSE*	*Covariates*
IDW	0.280	0.165	-	0.440	0.147	-	0.146	0.178	-
TPS	0.370	0.148	Elevation	0.423	0.150	Elevation	0.155	0.185	Elevation
GWR	0.270	0.150	Latitude	0.512	0.140	Latitude	0.152	0.183	Elevation Longitude
OK	0.490	0.137	-	0.470	0.145	-	0.090	0.180	-

Figure 2 shows the best geomechanical maps obtained through interpolation and the infiltration density additional predictor.

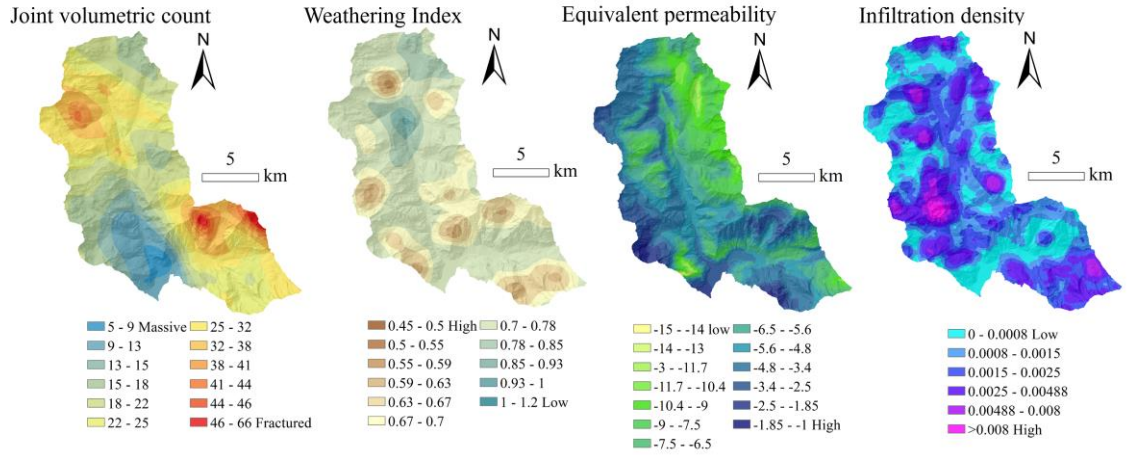

Figure 2. Geomechanical maps resulting from interpolations and infiltration density map.

4.2. Rockfall susceptibility model evaluation and performance assessment

The basic topographic model resulted in two penalized predictors, plan curvature and eastness, which were consequently not included in the successive geomechanical model.

Focusing on geomechanical predictors (figure 3a), J_v was described by a monotonic linear function, with higher susceptibility values corresponding to higher fracturing grades. This predictor explained about 10% of the model deviance. W_i and K_{eq} were penalized out of the model fitted on the entire data set and were associated to the lowest deviance explained for both around 7.5%. However, in some cross-validation runs, these predictors resulted in a not-penalized function. These results mean that these geomechanical properties influenced only slightly - or only locally when not penalized - rockfall occurrence in the area in comparison to the other predictors included in the analysis. However, the high uncertainty associated to K_{eq} regionalization would not exclude a possible different behaviour and influence of rock mass permeability on rockfalls (for instance, by calculating or calibrating this property based on *in situ* permeability tests, not available for the area).

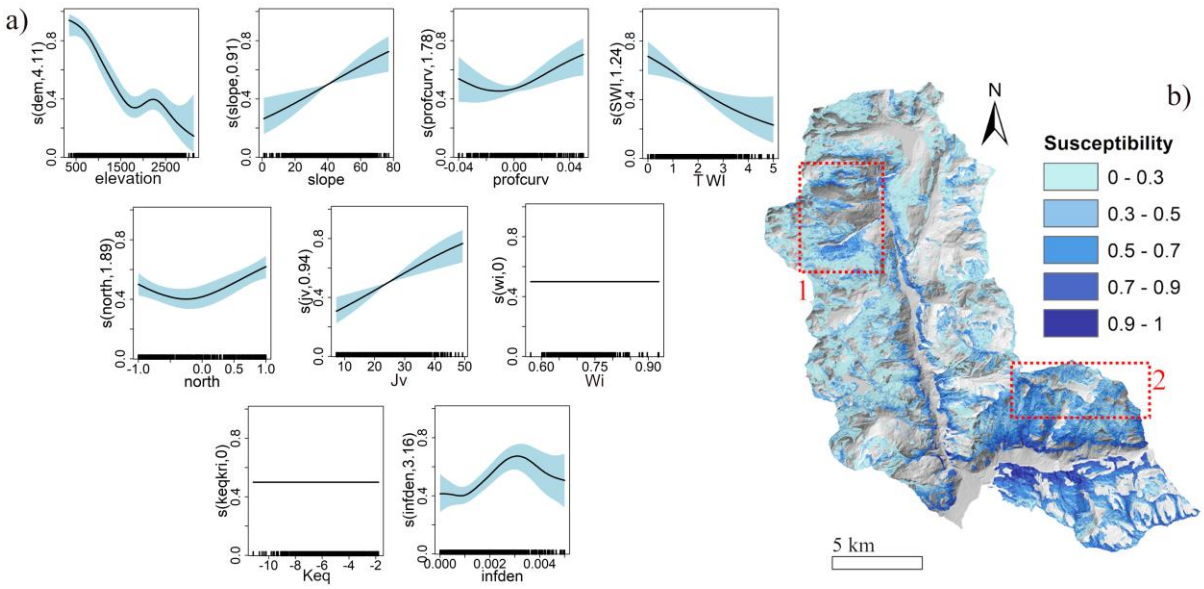

Figure 3. (a) predictors smooth functions with confidence bounds; (b) geomechanical model output susceptibility map. Red box represent the DSGSD area (1) and the regional thrust area (2).

Moreover, including climate-related predictors (e.g. rainfall and snow melting dynamics) could reshape the influence of K_{eq} in the susceptibility model, since the shape of the smoothing functions varies according to the predictors included in the analysis and the deviance explained by each of them.

Infiltration density, with a deviance explained around 10%, showed an increasing behavior in the first part of the smooth function and a slight decrease in correspondence of the highest predictor values. This inversion could be physically interpreted as slopes where a draining behavior prevails, with a consequent lower instability expected. The introduction of geomechanical predictors led to an increasing model performance in respect to the topographic model, with mean AUROC values from nsCV and sCV respectively of 0.77 and 0.71 for the test set; sCV is however to be preferred when dealing with spatial data, which are often subject to spatial autocorrelation [28]. The resulting susceptibility map coming from the geomechanical model is showed in figure 3b. Respect to the topography-based model, adding geomechanical predictors led to a susceptibility increment in two geomorphologically plausible contexts. The first one is in correspondence of the NW slope of San Giacomo Valley, characterized by complex DSGSD (Deep Seated Gravitational Slope Deformation) processes and the outcropping metasedimentary lithologies of the Spluga Syncline, associated to secondary instability and different deformation structures. The second is located around the regional thrust marking the contact between Tambò and Suretta nappes in the upper northern slope of Bregaglia Valley. Finally, the application of the geomechanical model using as train set only the IFFI inventory resulted in an opposite, not-physically plausible behaviour of the geomechanical predictors, especially J_v, and a concentration of high susceptibility values at the valley bottom. By testing the model on the additional inventory, the performance is lower than 0.7. These results were attributed to the fact that this official inventory was created in relation to element at risks and damages reported by administrations in charge, thus not totally representative of the environmental dynamics of the area.

5. Conclusions

Exploiting a rich geomechanical dataset for Chiavenna Valley (SO), this work was aimed at exploring the relationship between rock mass geomechanical properties and rockfall occurrence by means of generalized additive models. In particular, outcrop-scale geomechanical properties such as J_v, W_i and K_{eq}, and a hydro-geomorphological predictor, named infiltration density, were included in the analysis. Such predictors are time-consuming and difficult to collect and interpolate on large areas, thus rockfalls are usually linked to distance to fault or general bedding direction. The available dataset was updated with new several geomechanical surveys selected by a SSA sampling algorithm and different interpolation techniques were compared in order to create reliable maps for the geomechanical predictors. K_{eq} interpolation showed the scarcest performance, mainly due to the very local conditions of hydraulic aperture, which could change considerably even along the same outcrop. While J_v and infiltration density resulted to have a quite high influence in defining rockfall susceptibility, W_i and K_{eq} were penalized during the modelling procedure, meaning a slight – or only local - influence on susceptibility. This could be linked to a too site-specific connotation of these properties with rock mass instability, not generalizable to the whole study area. Compared to a simple topographic model, the introduction of geomechanical predictors led to a higher model performance, increasing susceptibility in geomorphologically plausible areas. In this study, the update of the rockfall inventory by means of detailed field survey, was crucial in avoiding inventory bias issues and physically unrealistic susceptibility maps.

Acknowledgments and funding

Authors would like to acknowledge the “Comunità Montana Valchiavenna” for the field survey permissions. This research was funded by MIUR PhD scholarship (XXXIV Cycle) and Erasmus+Traineeship.

References

[1] Scavia C, Barbero M, Castelli M, Marchelli M, Peila D, Torsello G and Vallero G 2020

Geosciences **10(3)**, 98
[2] Matasci B, Stock GM, Jaboyedoff M, Carrea D, Collins B D, Guérin A, Matasci G and Ravanel L 2018 *Landslides* **15** 859–78
[3] Coe J A and Harp E L 2007 *Nat. Hazards Earth Syst. Sci.* **7** 1–14
[4] Michoud C, Derron M-H, Horton P, Jaboyedoff M, Baillifard F-J, Loye A, Nicolet P, Pedrazzini A and Queyrel A 2012 *Nat. Hazards Earth Syst. Sci.* **12** 615–29
[5] Messenzehl K, Meyer H, Otto JC, Hoffmann T and Dikau R 2017 *Geomorphology* **287** 29–45
[6] Reichenbach P, Rossi M, Malamud B D, Mihir M and Guzzetti F 2018 *Earth-Science Reviews* **180** 60–91
[7] Ferrari F, Apuani T, Giani GP 2012 *GEAM* **135** 21-30.
[8] Ferrari F, Apuani T and Giani GP 2014 *International Journal of Rock Mechanics and Mining Sciences* **70** 162–76
[9] Pinheiro M, Vallejos J, Miranda T and Emery X 2016 *Engineering Geology* **205** 93–103
[10] Eivazy H, Esmaieli K and Jean R 2017 *Rock Mechanics and Rock Engineering* **50** 3175–95
[11] Ferrari F, Ziegler M, Apuani T and Loew S 2019 *Bull Eng Geol. Environ* **78**, 1645–68
[12] Brus DJ 2019 *Geoderma* **338** 464–80
[13] Zhou C, Yin K, Cao Y, Ahmed B, Li Y, Catani F and Pourghasemi HR 2018 *Computers & Geosciences* **112** 23–37
[14] Fanos AM and Pradhan B 2019 *Earth Systems and Environment* **3** 491–506
[15] Bieniawski Z T 1973 *Civil Engineer in South Africa* **15** 343-53
[16] Barton N, Reidar L and Lunde J 1974 *Rock mechanics* **6** 189-236.
[17] Goetz J, Brenning A, Petschko H and Leopold P 2015 *Comput. Geosci* .**81** 1-11
[18] Galli A, Le Bayon B, Schmidt MW, Burg J-P, Reusser E 2013 *Swiss Journal of Geosciences* **106** 33–62
[19] Tantardini D, Riganti N, Taglieri P, De Finis E, Bini A 2013 *Alpine and Mediterranean Quaternary* **26** 77-94
[20] Tantardini D *PhD Thesis* Geologia del quaternario e geomorfologia della bassa valchiavenna (SO) Università degli Studi di Milano Milano – Dip. Scienze della Terra A. Desio (XXVIII cycle, A.Y. 2015).
[21] Van Groenigen JW, Siderius W, Stein A 1999 *Geoderma* **87** 239–594
[22] Deere, D.U. and Miller, R.P. 1966. Engineering classification and index properties of rock. Technical Report No. AFNL-TR-65-116. Albuquerque, *NM: Air Force Weapons Laboratory*
[23] Stahl T, Winkler S, Quigley M, Bebbington M, Duffy B and Duke D 2013 *Earth Surf. Process. Landforms* **38** 1838-50.
[24] Kiraly L 1969 *Geol. Helv.* **62/2** 613–619.
[25] Coli N, Pranzini G, Alfi A, Boerio V 2008 *Engineering Geology* **101** 174–84
[26] Knevels R, Petschko H, Proske H, Leopold P, Maraun D and Brenning 2020 *Geosciences* **10(6)** 217.
[27] Wood SN 2017 Generalized Additive Models: An Introduction with R 2nd ed (Boca Raton, FL, USA: Chapman and Hall/CRC)
[28] Brenning A 2005 *Nat. Hazards Earth Syst. Sci*. **5** 853–862